10.1071/CH14561_AC

Australian Journal of Chemistry, 2015, 68 (7), 1076-1083

Supplementary Material

pH-Dependent various copper (II) coordination architectures constructed from *N,N'*-di(3-pyridyl)succinamide and two different dicarboxylates

Xiu–li Wang*, Fang–fang Sui, Hong–yan Lin, Guo–cheng Liu

Department of Chemistry, Bohai University, Liaoning Province Silicon Materials Engineering Technology Research Centre, Jinzhou 121000, People's Republic of China

Table S1. Selected bond distances (Å) and angles (deg) for compound **1**

Cu(1)-O(3)#1	1.959(4)	Cu(1)-N(1)#1	1.999(4)
Cu(1)-O(3)	1.959(4)	Cu(1)-N(1)	1.999(4)
O(3)#1-Cu(1)-O(3)	86.8(2)	O(3)#1-Cu(1)-N(1)	92.03(17)
O(3)#1-Cu(1)-N(1)	166.26(19)	O(3)-Cu(1)-N(1)	166.26(19)
O(3)-Cu(1)-N(1)#1	92.03(17)	N(1)#1-Cu(1)-N(1)	92.3(2)

Symmetry code for (a) #1 -x+1, y, -z+1/2

Table S2. Selected bond distances (Å) and angles (deg) for compound **2**

Cu(1)-O(3)	1.9065(17)	Cu(1)-N(4)#1	2.080(2)
Cu(1)-O(5)	1.9105(17)	Cu(1)-N(1)	2.099(2)
O(3)-Cu(1)-O(5)	175.75(7)	O(3)-Cu(1)-N(1)	89.05(7)
O(3)-Cu(1)-N(4)#1	91.62(7)	O(5)-Cu(1)-N(1)	89.31(8)
O(5)-Cu(1)-N(4)#1	90.09(8)	N(4)#1-Cu(1)-N(1)	178.69(7)

Symmetry code for (a) #1 x-1, y+1, z

* Corresponding author. Tel: +86-416-3400158, Fax: +86-416-3400158.

E-mail address: wangxiuli@bhu.edu.cn (X.L. Wang).

Table S3. Selected bond distances (Å) and angles (deg) for compound **3**

Cu(1)-O(3)	1.9384(17)	Cu(1)-N(4)#2	2.022(2)
Cu(1)-O(7)#1	1.9816(17)	Cu(1)-N(1)	2.032(2)
O(3)-Cu(1)-O(7)#1	165.62(8)	O(3)-Cu(1)-N(1)	91.42(8)
O(3)-Cu(1)-N(4)#2	91.88(8)	O(7)#1-Cu(1)-N(1)	89.19(8)
O(7)#1-Cu(1)-N(4)#2	90.86(8)	N(4)#2-Cu(1)-N(1)	166.42(9)
Symmetry code for (a)#1 x, y+1, z		(b) #2 x+1, y-1, z-1	

Table S4. Selected bond distances (Å) and angles (deg) for compound **4**

Cu(1)-N(1)#1	1.989(4)	Cu(2)-N(3)#2	1.997(4)
Cu(1)-N(1)	1.989(4)	Cu(2)-N(3)	1.997(4)
Cu(1)-O(3)	2.012(4)	Cu(2)-O(5)#2	1.998(4)
Cu(1)-O(3)#1	2.012(4)	Cu(2)-O(5)	1.998(4)
N(1)#1-Cu(1)-N(1)	179.998(1)	N(3)#2-Cu(2)-N(3)	180
N(1)#1-Cu(1)-O(3)	90.62(16)	N(3)#2-Cu(2)-O(5)#2	89.16(16)
N(1)-Cu(1)-O(3)	89.38(16)	N(3)-Cu(2)-O(5)#2	90.84(16)
N(1)#1-Cu(1)-O(3)#1	89.38(16)	N(3)#2-Cu(2)-O(5)	90.84(16)
N(1)-Cu(1)-O(3)#1	90.62(16)	N(3)-Cu(2)-O(5)	89.16(16)
O(3)-Cu(1)-O(3)#1	179.999(1)	O(5)#2-Cu(2)-O(5)	179.999(1)
Symmetry code for (a) #1 -x+2, -y+2, -z; (b)#2 -x+3, -y+1, -z+1			

Table S5. Hydrogen-bonding geometry (Å, °) for compound **2**

D–H···A	D–H	H···A	D···A	D–H···A
N(2)–H(2B)···O(1W)[a]	0.86	1.93	2.7895	176
O(1W)–H(1WA)···O(2)[b]	0.68	2.17	2.8334	166
Symmetry code for (a) 1+x, y, z; (b) 1-x, -y, 1-z				

Table S6. Hydrogen-bonding geometry (Å, °) for compound **3**

D–H···A	D–H	H···A	D···A	D–H···A

N(2)–H(2B)···O(13)[a]	0.86	2.04	2.8809	166

Symmetry code for (a) -x, 1-y, -z

Table S7. Hydrogen-bonding geometry (Å, °) for compound **4**

D–H···A	D–H	H···A	D···A	D–H···A
N(2)–H(2B)···O(3)[a]	0.86	2.07	2.9287	173

Symmetry code for (a) -1+x, y, z

Table S8. Conformations of ligand **L** and corresponding angles for compounds **1-4**

Compounds	Diagram of L	C–C–C–C Torsion angle/°	Conformation
1	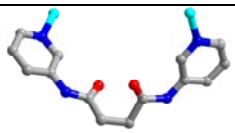	63.37	cis
2	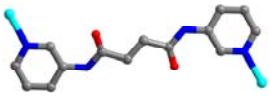	-173.91	trans
3	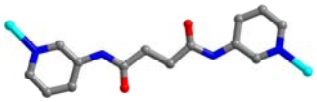	-175.80	trans
4	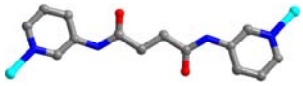	-180.00	trans

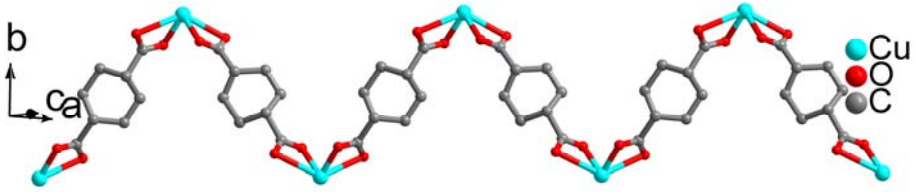

(a)

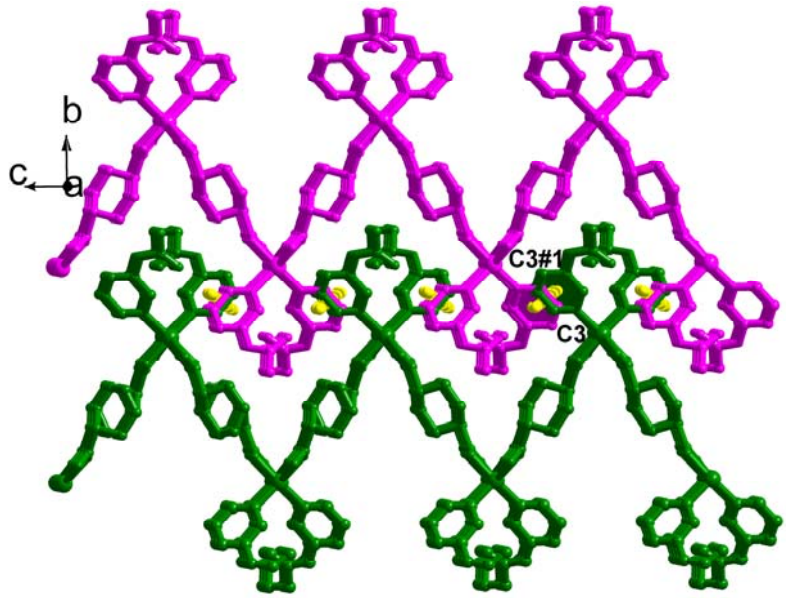

(b)

Fig. S1 (a) The 1D $[Cu\text{-}1,4\text{-}chdc]_n$ zigzag chain in **1**. (b) The 3D supramolecular network formed by π–π stacking interactions in **1**.

(a)

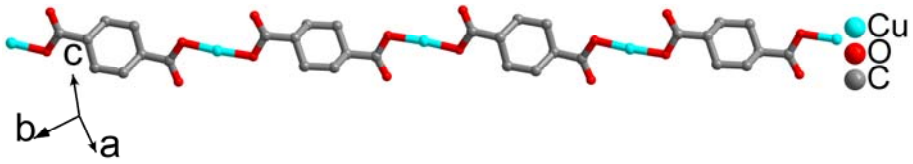

(b)

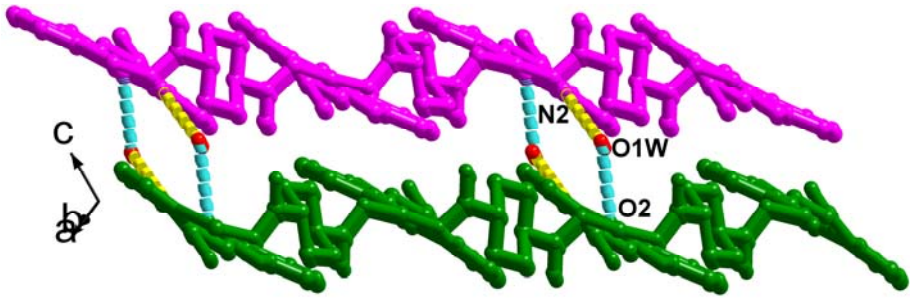

(c)

Fig. S2 (a) The 1D $[Cu\text{-}\mathbf{L}]_n$ zigzag chain in **2**. (b) The 1D linear $[Cu\text{-}1,4\text{-}chdc]_n$ chain in **2**. (c) View of 3D supramolecular architecture formed by hydrogen-bonding interactions in **2**.

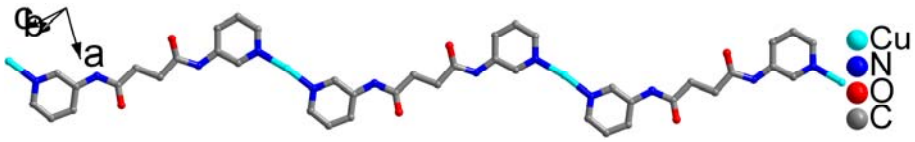

(a)

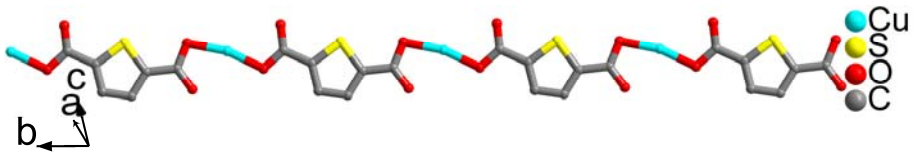

(b)

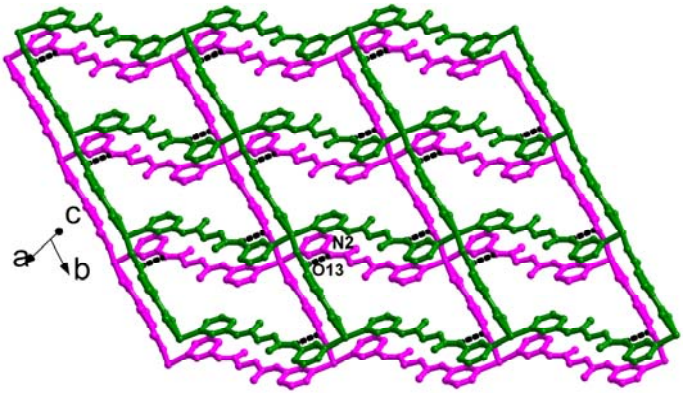

(c)

Fig. S3 (a) The 1D [Cu-**L**]$_n$ zigzag chain in **3**. (b) The 1D linear [Cu-2,5-tdc]$_n$ chain in **3**. (c) View of 3D supramolecular architecture formed by hydrogen-bonding interactions in **3**.

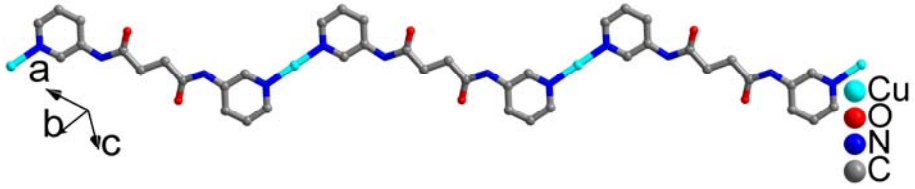

(a)

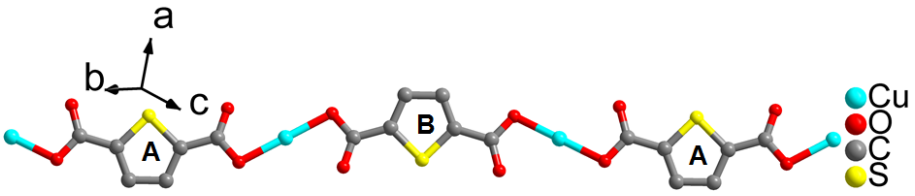

(b)

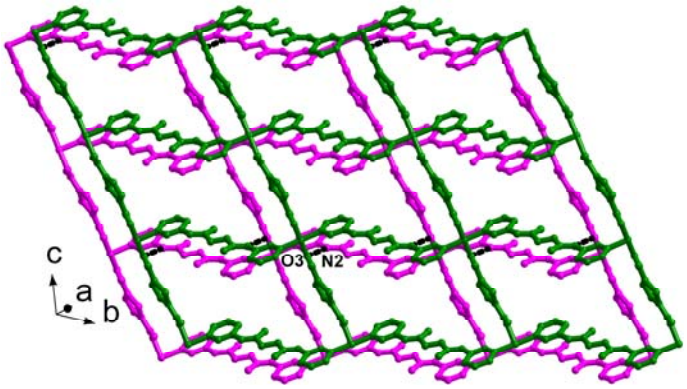

(c)

Fig. S4 (a) The 1D $[Cu\text{-}\mathbf{L}]_n$ zigzag chain in **4**. (b) The 1D linear ABAB $[Cu\text{-}2,5\text{-}tdc]_n$ chain in **4**. (c) View of 3D supramolecular architecture formed by hydrogen-bonding interactions in **4**.

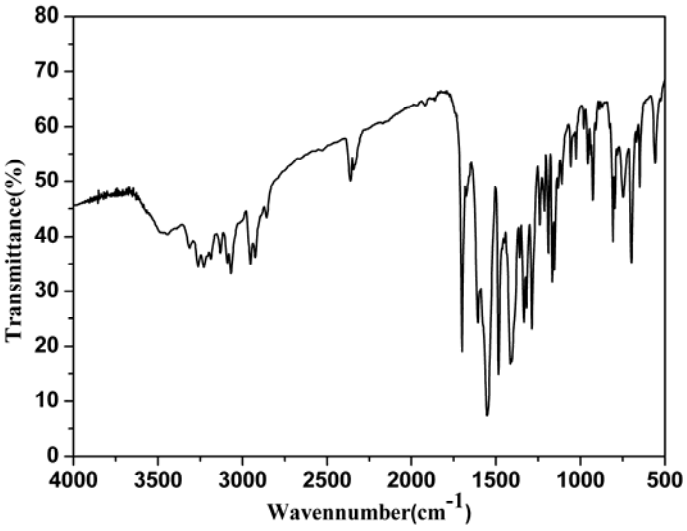

(a)

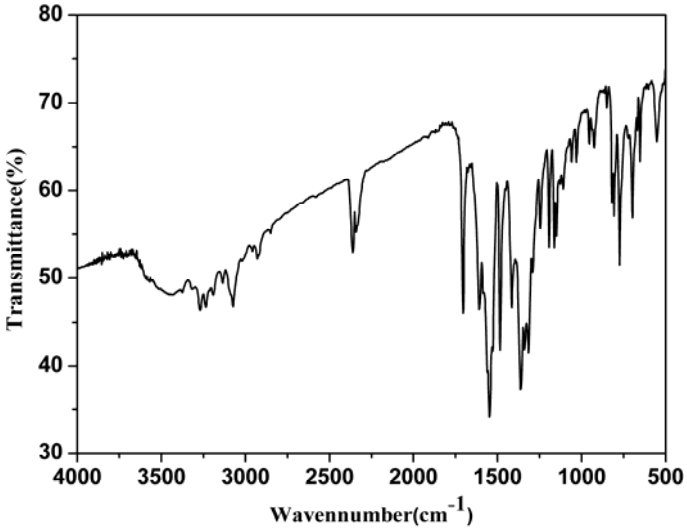

(b)

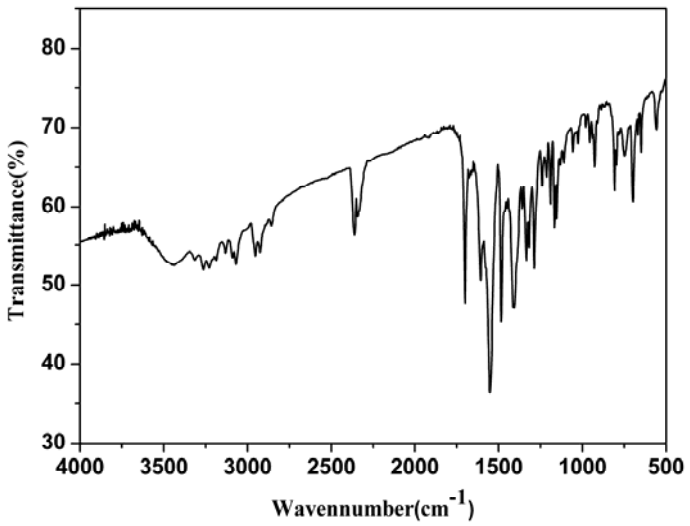

(c)

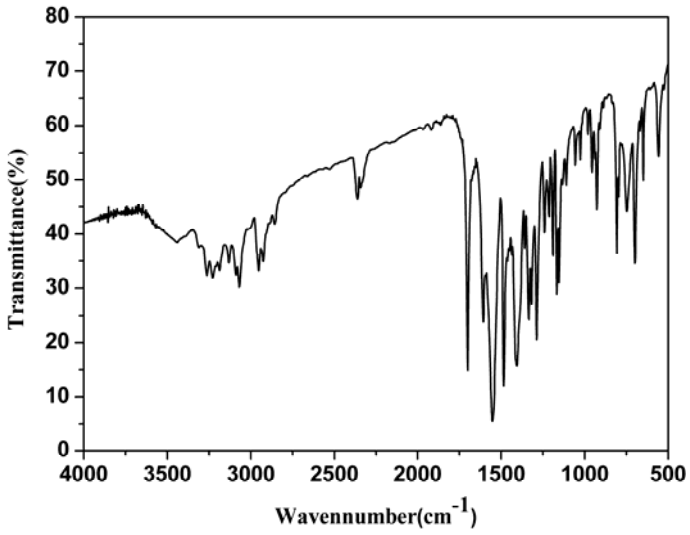

(d)

Fig. S5 IR spectra for compounds **1**-**4**.

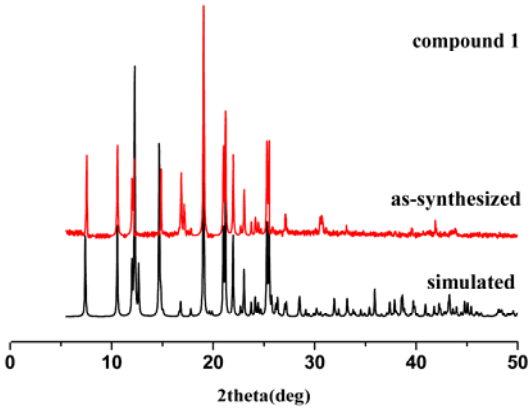

(a)

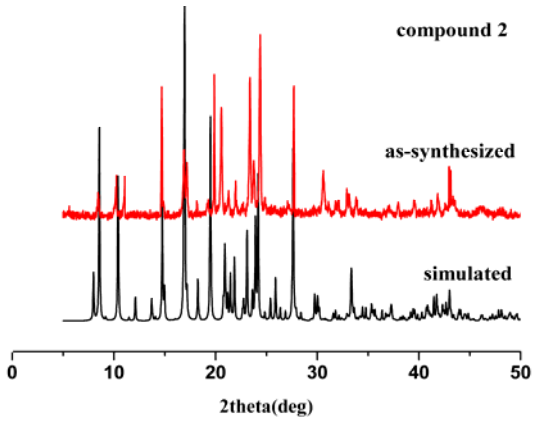

(b)

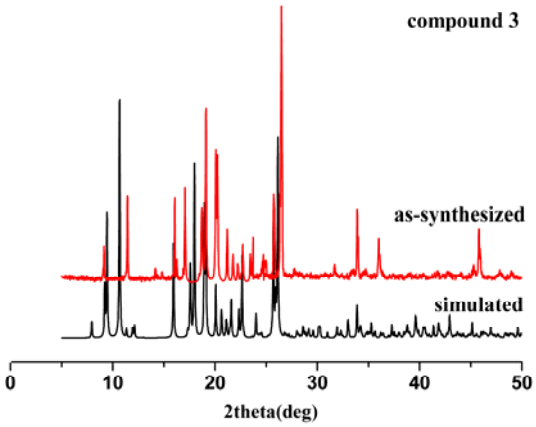

(c)

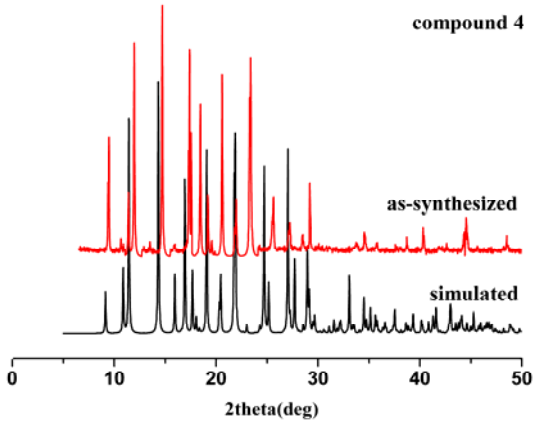

(d)

Fig. S6. The simulated (black line) and fresh samples (red line) powder X–ray diffraction patterns for compounds **1**–**4**.

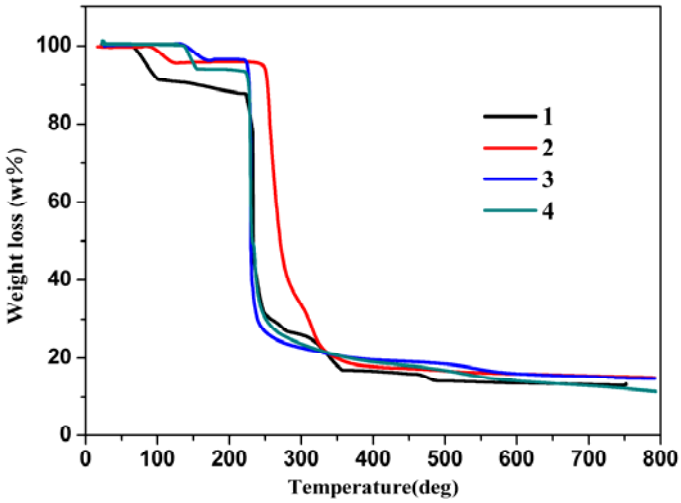

Fig. S7. TGA curves for compounds **1**–**4**.

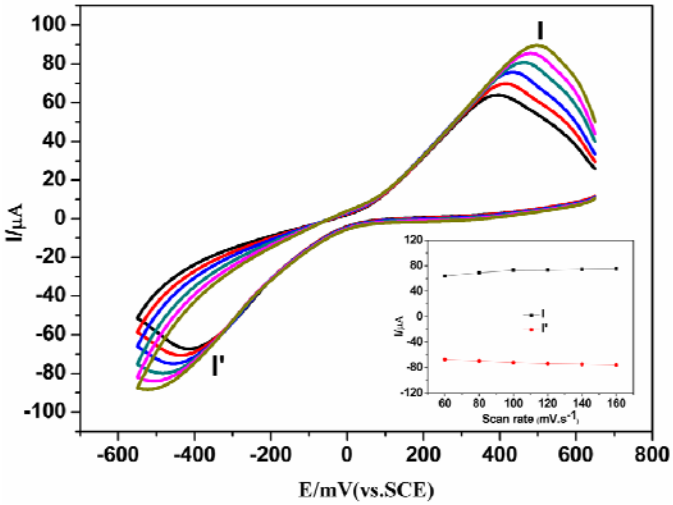

Fig. S8. Cyclic voltammograms of the **2**-CPE in 0.1 mol·L^{-1} H_2SO_4 + 0.5 mol·L^{-1} Na_2SO_4 solution at different scan rates (from inner to outer: 60, 80, 100, 120, 140, 160 mV·s^{-1}). The inset shows the plots of the anodic and cathodic peak currents against scan rates.

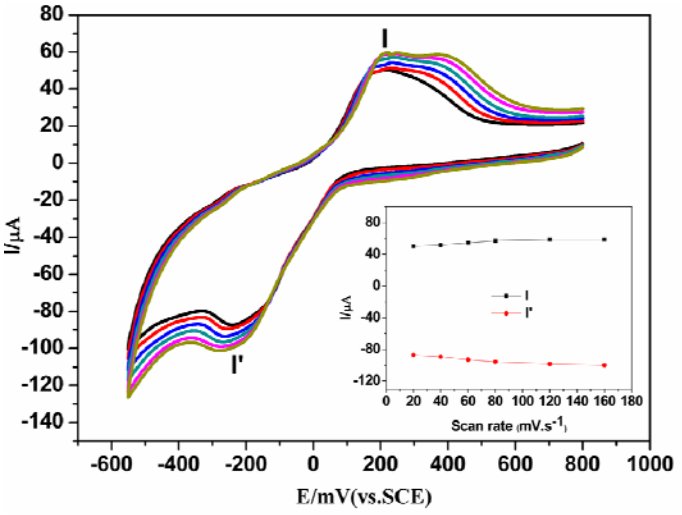

Fig. S9. Cyclic voltammograms of the **3**-CPE in 0.1 mol·L^{-1} H_2SO_4 + 0.5 mol·L^{-1} Na_2SO_4 solution at different scan rates (from inner to outer: 20, 40, 60, 80, 100, 120, 140, 160 mV·s^{-1}). The inset shows the plots of the anodic and cathodic peak currents against scan rates.

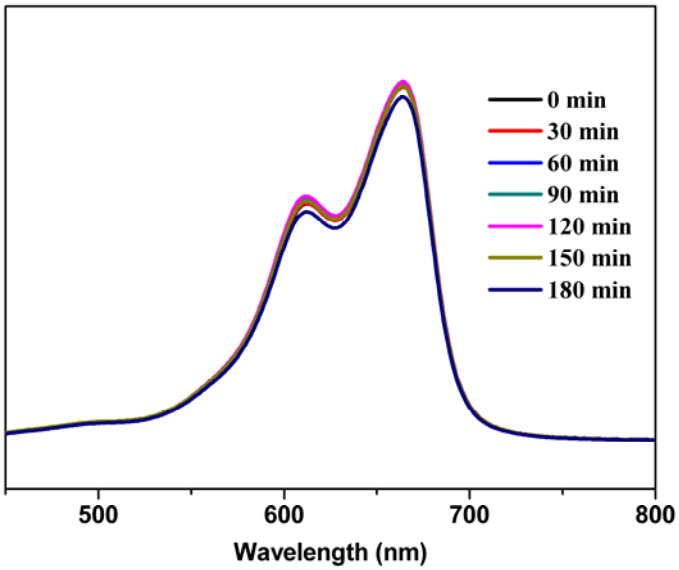

Fig. S10. Absorption spectra of the MB solution during the decomposition reaction under UV light irradiation with the use of compound **2**.

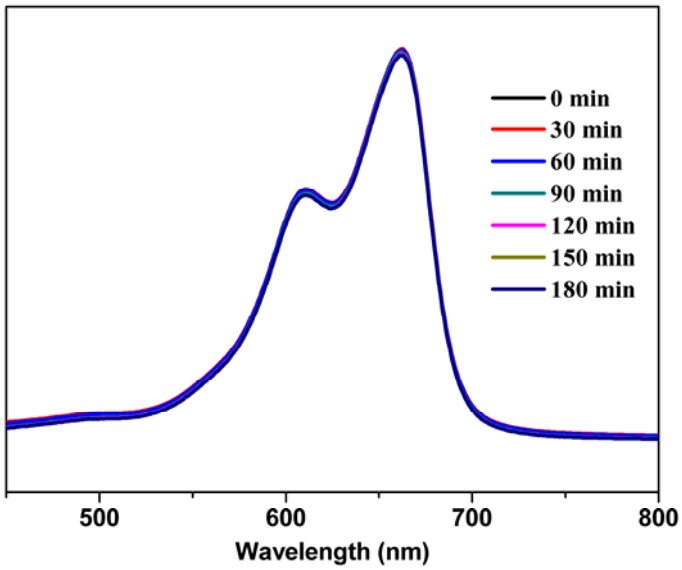

Fig. S11. Absorption spectra of the MB solution during the decomposition reaction under UV light irradiation with the use of compound **3**.

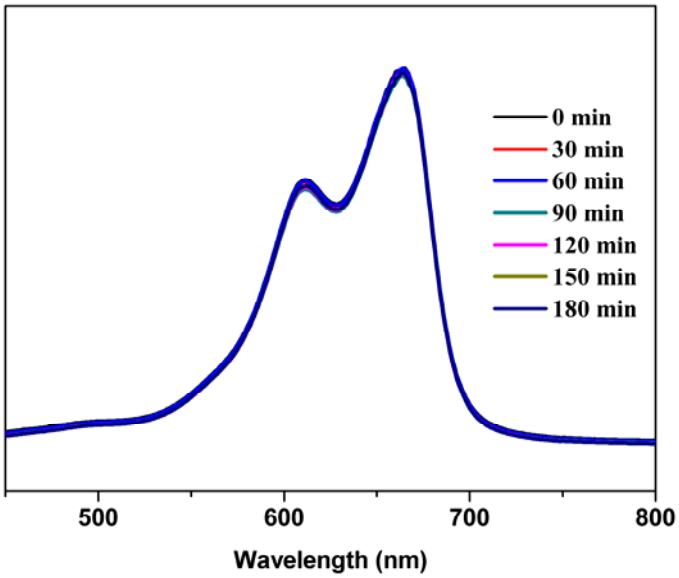

Fig. S12. Absorption spectra of the MB solution during the decomposition reaction under UV light irradiation with the use of compound **4**.

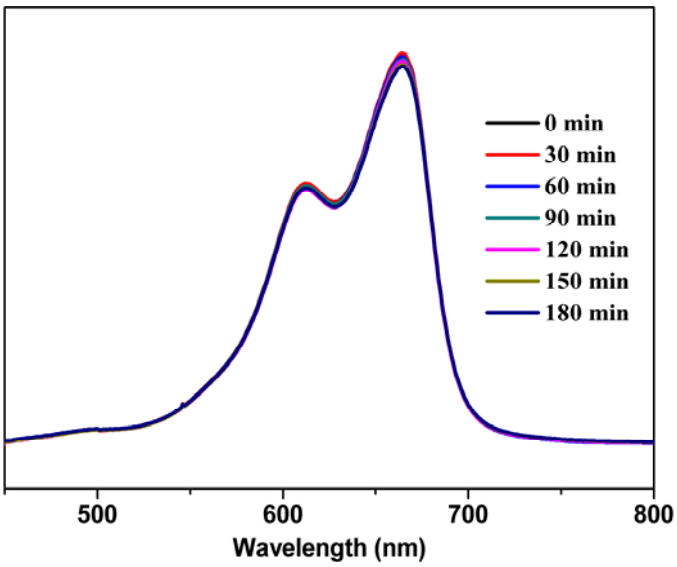

Fig. S13. Absorption spectra of the MB solution during the decomposition reaction under UV light irradiation without crystal in the same conditions.